ORIGINAL PAPER

Theoretical design, synthesis, characterization and solvatochromic studies and non-linear optical properties of poly[(2,3,5,6- tetrafluorop henyl)-2,3-dihydrothieno[3,4-b][1,4]dioxine)] copolymer

Anju Maria Baby[1] · Anugop Balachandran[2] · Madanan Kailasnath[2] · Krishnapillai Sreekumar[1]

Abstract

A donor–acceptor type π-conjugated conducting, poly[(2,3,5,6- tetrafluorophenyl)-2,3-dihydro-thieno[3,4-b][1,4]dioxine)], P(EDOT-4FPH) was designed and synthesized by direct arylation polymerization method. Computational calculations for the monomers, oligomers, and copolymer were performed using Gaussian 09 with two hybrid functional, B3LYP and HSE06 using (6-31G (d,p)) basis set. Theoretical band gap obtained from HSE06 (6-31G/d,p) basis set was 2.94 eV. The polymer was characterized by FTIR, ^{1}H NMR, EDX, and TGA. The Electrochemical band gap was determined by cyclic voltammetry (CV), differential pulse voltammetry (DPV), and square wave voltammetry (SWV). The values were 1.81 eV,1.71 eV and 1.64 eV. Optical band gap was observed to be 2.05 eV. Photophysical studies were performed and the copolymer exhibited lifetime decay of 0.55 ns and quantum yield of 0.37 in chloroform solution. It showed positive solvatochromism with a large Stoke's shift from 2310 cm^{-1} to 4152 cm^{-1} in solutions of varying polarity. Third-order non-linear optical properties of the copolymer P(EDOT-4FPH) were observed using the open-aperture Z-scan technique at 532 nm in DMSO solvent. OA Z-scan trace and optical limiting effect of the copolymer were studied at different laser intensities. At 10 μJ, the lowest optical threshold of 0.005 GW/cm^2 was found with reverse saturable non-linear absorption and non-linear absorption coefficient of 3.63×10^{-9} m/W.

Introduction

During the last three decades, organic conducting polymers have found varied applications as photocatalysts [1], biosensors [2, 3], electrochromic materials [4], optoelectronic devices [5] etc. due to their fascinating advantages such as low cost, ease of fabrication, processability, high optical contrast, and high thermal stability [6]. Several systematic procedures have been proposed to bring out the increased absorption range of these polymers, with one of the most fruitful being the "push–pull" structure, where alteration of electron-releasing and electron-withdrawing groups represent an outstanding way to tune the HOMO and LUMO energy levels of a conjugated system. The introduction of electron-donor groups was effective in raising the HOMO level. Thus the donor unit dominates the HOMO of the copolymer, whereas, LUMO is predominant by the acceptor unit, thereby lowering the optical bandgap [7, 8]. Recently, 3,4-ethylenedioxythiophene based organic materials have emerged as one of the most relevant compounds which seem to have potential applications in diode components, field-effect transistors, flexible electroluminescent lamps, organic solar cells, nonlinear optical devices, organic LED, and other devices due to their easiness of synthesis, high ionization potential, high charge carrying mobility, environmental stability, and the possibility to modify them with different chemical groups [9–16]. Certain thiophene-based

✉ Krishnapillai Sreekumar
   kskpolymer.cusat@gmail.com

   Anju Maria Baby
   anjumaria9@gmail.com

[1] Department of Applied Chemistry, Cochin University of Science and Technology, Kochi 22, Kerala, India

[2] International School of Photonics, Cochin University of Science and Technology, Kochi 22, Kerala, India

organic materials are, Ethylenedioxythiophene (EDOT), Bithiophene, Propylenedioxythiophene (ProDOT), 3-Methylthiophene, etc. The present work deals with the synthesis of a Donor–Acceptor type copolymer, where EDOT mainly plays the role of donor and tetrafluorobenzene acts as the acceptor. Nitti et al.synthesized D-A type copolymers with 1,2,4,5-tetrfluorobenzene as the acceptor unit and 2,5 dialkoxybenzene or benzodithiophene as donor units [17]. The planar and electron-deficient nature of tetrafluorobenzene makes it applicable for constructing polymers and the presence of fluorine atoms helps to gain more thermal and oxidative stability along with hydrophobicity [16, 18–20].

Direct arylation polymerization method was adopted to synthesize the copolymer EDOT-tetrafluobenzene P(EDOT-4FPH) [21–26] which was considered as a novel approach for the synthesis of organic π conjugated polymers. Recently, EDOT based D-A type copolymers were reported, synthesized by direct arylation method that includes EDOT incorporated with anthracene, bithiophene and triphenylamine units [27], EDOT- chalcogenadiazole [28] and EDOT-Quinoxaline based copolymers [29]. Also, direct arylation method was employed to synthesize tetrafluorobenzene based polymers in combination with biphenol [30] and thiophene based monomers [31] and oligomer units [32]. This method is very much productive for constructing Ar–Ar compounds by the coupling of aryl halides with catalytically activated C-H bonds of the corresponding monomers. The major benefits of the direct arylation polymerization technique are; easy synthetic steps, economically attractive, less rigorous polymerization conditions, relatively high yield, and could synthesize polymers with amazing charge transport properties.

The present article deals with the theoretical investigations of EDOT and tetraflurobenzene [33], donor–acceptor units, and the polymer which were used to evaluate the electronic and optical properties by employing Gaussian 09. Synthesis, thermal stability, electrochemical and photophysical properties were also examined. Third-Order Nonlinear optical properties of the copolymer are discussed and demonstrated.

Experimental

Materials

3,4-Ethylenedioxythiophene (Aldrich, 98%), tetrafluorobenzene (Aldrich), tricyclohexylphosphine tetrafluoroborate (Spectrochem Pvt. Ltd), N-bromosuccinimide (SRL), Sodium Chloride (Isochem), diethyether (Spectrochem Pvt. Ltd), Magnesium sulphate (anhydrous), Pivalic acid (Spectrochem Pvt. Ltd), Pottasium carbonate (Merck), Palladium acetate (Spectrochem Pvt. Ltd), were used as received.

Dimethylacetamide (anhydrous) (DMAc, Spectrochem Pvt. Ltd), Chloroform ($CHCl_3$, Spectrochem Pvt. Ltd), Dimethyformamide (DMF, Spectrochem Pvt. Ltd), Methanol (Spectrochem Pvt. Ltd), Tetrahydrofuran, (HPLC grade, Spectrochem Pvt. Ltd), n-Hexane, (Spectrochem Pvt. Ltd), Ethylacetate (Spectrochem Pvt. Ltd), Toluene, Acetonitrile (CH_3CN, Spectrochem Pvt. Ltd), Acetone (Spectrochem Pvt. Ltd), were dried and distilled when necessary according to the standard procedures.

Computational methods

The electronic structure, properties and energy band gap of the copolymer P(EDOT-4FPH) and the oligomer units were investigated using density functional theory (DFT) calculations, carried out with Gaussian 09 with two hybrid functionals B3LYP (Becke,three parameter, Lee–Yang–Parr) [34–36] and HSEh1PBE referred to as HSE06 (full Heyd-Scuseria-Ernzerh of functional) at 6-31G (d,p) basis set [37–46]. Electronic properties of the copolymer P(EDOT-4FPH) were studied by the Periodic Boundary Condition (PBC) calculations. Band structure of the copolymer in the positive region of the first Brillouin zone (between k = 0 and k = π/a) was plotted like in the previous reports [28, 29].

Synthesis procedures

2,5–Dibromo-3,4-ethylenedioxythiophene

To a solution of EDOT (14.1 mmol) in DMF (20 ml) was added N-Bromosuccinimide (28.2 mmol). The reaction mixture was stirred for 1 h at room temperature. The resulting slurry was poured into water and extracted with diethyl ether, brine solution was used for washing the organic fractions and dried over Magnesium sulphate. The solvent was removed under reduced pressure. By column chromatographic technique, the white solid was purified using n-hexane as eluent [47]. GCMS ($M^{+)}$ = 299, (Fig. S1 supporting information), M.P = 95-98^{0}C, ^{1}H NMR (400 MHz, CDCl$_3$) δ = 4.27 (s, 4H) (Fig. S2 supporting information).

Synthesis of P(EDOT-4FPH)

To a 3 necked RB flask containing DMAc (20 ml) solvent that was purged with nitrogen, K_2CO_3 (3 mmol), Pd(OAc)$_2$ (0.04 mmol), PCy$_3$.BF$_4$ (0.08 mmol), Pivalic acid (0.6 mmol) were added. Tetrafluorobenzene (1 mmol), and 2,5-dibromo-3,4-ethylenedioxythiophene (1 mmol) were added to the reaction mixture. The reaction mixture was stirred at 100^{0}C for 48 h and was cooled to room temperature. The mixture was added to ice-cold methanol. The precipitate was filtered and washed with methanol. The polymer

was purified by soxhlet extraction using hexane and methanol for 24 h. The residue was dried under vaccum. [9, 21, 48–52].

Instrumentation

The molecular weight of the monomers was determined by GC–MS analysis using 1200 L single quadrupole, Varian gas chromatograph model using Helium as the carrier gas. [1]H Nuclear magnetic resonance (^{1}H NMR) spectra of the copolymer EDOT-4FPH and the monomers were recorded with a Bruker Avance III (400 MHz) spectrometer, and chemical shifts were recorded in δ units with downfield of TMS as the internal standard. Perkin Elmer Spectrum 100, FT-IR Spectrometer recorded the Fourier transform Infra-Red (FT-IR) spectrum using KBr pellets. The copolymer was further characterized by Absorption and Fluorescence spectra, recorded with Thermo Scientific, Evolution 201, Ultraviolet–Visible (UV–Visible) spectrophotometer and Horiba Fluorolog-3, Steady-State Fluorescence Spectrometer respectively. Electrochemical measurements were performed in dry acetonitrile with Bu_4NPF_6 (0.10 M) as the supporting electrolyte at room temperature under nitrogen atmosphere. A thin polymer film coated on the platinum electrode performed as the working electrode, the role of counter and reference electrodes were executed by Pt wire and Ag/Ag + electrodes respectively, using CH Instruments Electrochemical workstation with a quiet time of 2 s and scan rate of 100 mV/s. Thermogravimetric (TG and DTG) measurements were performed using Perkin Elmer Diamond 6 instrument under nitrogen atmosphere at a heating rate of 10 °C/min. Molecular weight and polydispersity index of the copolymers were determined by Gel Permeation Chromatography (GPC) using Prominence Series Shimadzu instrument with polystyrene gel 5 µm 10E4Å using THF as the eluent. Horiba Fluorolog-3 Time-correlated single-photon counting system (TCSPC) measured fluorescence lifetime. Fluorescence lifetime values were determined by deconvolution of the data with exponential decay using DAS6 decay analysis software. Third-order nonlinear optical measurements were carried out by using single beam Z-scan technique with Nd: YAG laser system with pulse width of 6 ns at 10 Hz repetition rate and 532 nm as in the previously reported EDOT based polymers [27–29].

Results and discussion

Theoretical calculations

Using Density functional theory (DFT) calculations, the geometries of the monomers, Donor–Acceptor units of 3,4-ethylenedioxythiophene and 1,2,4,5-tetrafluorobenzene

and the copolymer P(EDOT-4FPH) were optimized with the assistance of B3LYP/6-31G (d,p) and HSE06/6-31G (d,p) basis set. HOMO energy level was calculated as the highest level of occupied molecular orbitals and LUMO energy level was calculated as the lowest level of unoccupied molecular orbitals. The HOMO, LUMO energy levels were calculated and predicted the band gap of 2,5-dibromo-3,4-ethylenedioxythiophene and tetraflurobenzene, D-A units and the corresponding copolymer. The images of HOMO, LUMO energy levels and the optimized geometries obtained from the theoretical calculations are shown in Table 1.

From the values obtained from the two-hybrid functionals, for the HOMO, LUMO energy levels of the monomers, it was revealed that the LUMO level of 1,2,4,5 tetrafluorobenzene was lower in comparison with that of 2,5-dibromo-3,4-ethylenedioxythiophene. To be exact, -0.84 eV and –1.02 eV were the LUMO values observed by B3LYP/6-31G (d,p) and HSE06/6-31G (d,p) methods respectively. Lower the LUMO value, more will be the acceptor strength of the unit. Here, tetrafluorobenzene was a good acceptor while the ethylenedioxythiophene executed the role of the donor. The energy level diagrams achieved by employing the two methods are illustrated in Figs. 1 and 2. In both situations, there observed a reduction in the band gap from monomer to oligomer units and finally to the copolymer. By B3LYP/6-31G (d,p) method, 4.04 eV, 3.86 eV,3.60 eV, 3.46 eV, and 3.34 eV were the band gaps calculated for EDOT-4FPH, $(EDOT-4FPH)_2$, $(EDOT-4FPH)_3$, $(EDOT-4FPH)_4$, and $P(EDOT-4FPH)_n$ respectively. It was revealed that the band gap was reduced by 0.70 eV from the single donor–acceptor unit to the copolymer. It came out with a similar pattern in the second method HSE06, where the band gaps were found to be 4.08 eV, 3.48 eV, 3.22 eV, 3.08 eV, and 2.94 eV which corresponded to the single, dimer, trimer, tetramer donor–acceptor units and finally the copolymer. But there was a notable difference in the band gap reduction which seemed to be a factor of 1.14 eV; in other words, more reduction was observed in the case of HSE06/6-31G (d,p) when compared with the B3LYP/6-31G (d,p) method. Comparing with the previous reports, P(EDOT-FL) [53] showed band gap of 3.12 eV and 3.51 eV by HSE06/6-31G (d,p) and B3LYP/6-31G (d,p) methods respectively, which are higher than the band gap values of P(EDOT-4FPH) and the results are comparable with the reported copolymer where triphenylamine act as the acceptor unit [27] by both methods.

By incorporating tetrafluorobenzene to the 3,4-ethylenedioxythiophene unit, there occurred a decrease in the band gap from monomer units to the single donor–acceptor unit and to the polymer due to the increased delocalization of electrons over the conjugated polymeric backbone. This was confirmed from the frontier molecular orbital distribution (Table 1) where

Table 1 Optimised geometry and HOMO, LUMO energy levels of P(EDOT-4FPH) by HSE06/6-31G (d,p) basis set
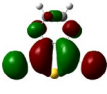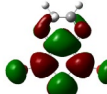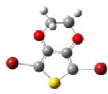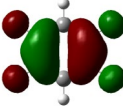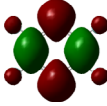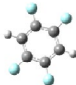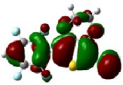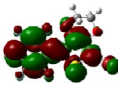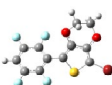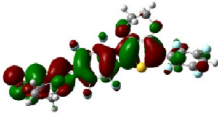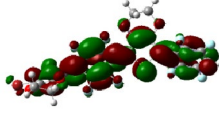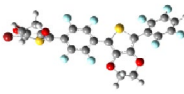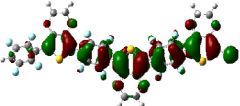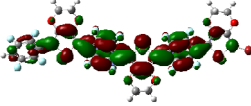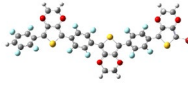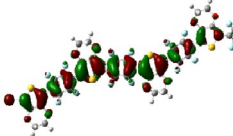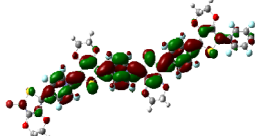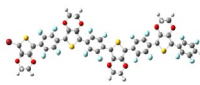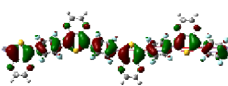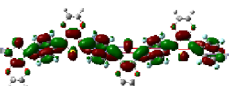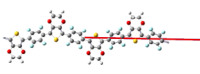
D-A units	HOMO	LUMO	Optimised geometry
Br-EDOT-Br			
4FPH			
EDOT-4FPH			
(EDOT-4FPH)$_2$			
(EDOT-4FPH)$_3$			
(EDOT-4FPH)$_4$			
P(EDOT-4FPH)$_n$			

Fig. 1 Energy level diagram of EDOT-4FPH, (EDOT-4FPH)$_2$, (EDOT-4FPH)$_3$, (EDOT-4FPH)$_4$, and P(EDOT-4FPH)$_n$ by HSE06/6-31G (d,p)
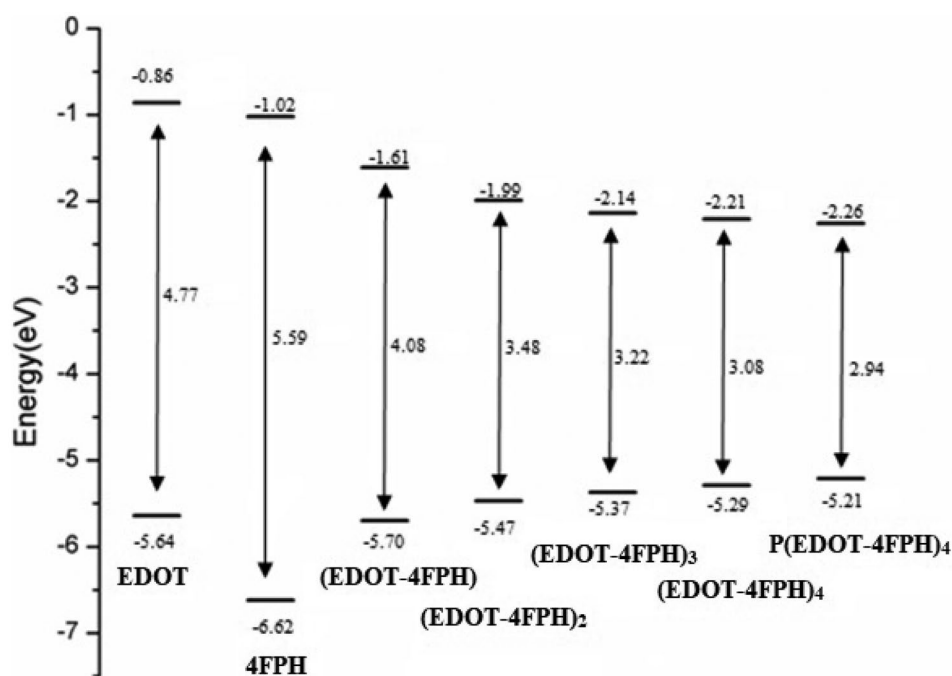
HOMO level and LUMO level were spread over the entire D-A unit. The reduction in band gap got increased, as it went from a single D-A unit to the polymer.

Optimized unit cell geometry of the polymer is shown in Fig. 3 and the red line started from the centre part of the tetramer symbolize the translational vector of length 32.52 A^0, in such a way that the optimized unit cell geometry gets repeated exactly along the translational vector in countless numbers. Final coordinates and the translational vectors

of the optimized geometry of the copolymer by both the methods HSE06/6-31G (d,p) and B3LYP/6-31G (d,p) are given in the (supporting information Tables S1 and S2).

Structural characterization

The procedure for the synthesis of the monomer 2,5-dibromo-3,4-ethylenedioxythiophene is illustrated in Scheme 1 and the copolymer P(EDOT-4FPH) was

Fig. 2 Energy level diagram of EDOT-4FPH, (EDOT-4FPH)$_2$, (EDOT-4FPH)$_3$, (EDOT-4FPH)$_4$, and P(EDOT-4FPH)$_4$ by B3LYP/6-31G (d,p)

Fig. 3 Unit cell for the PBC HSE06/6-31G (d,p) calculation of P(EDOT-4FPH)

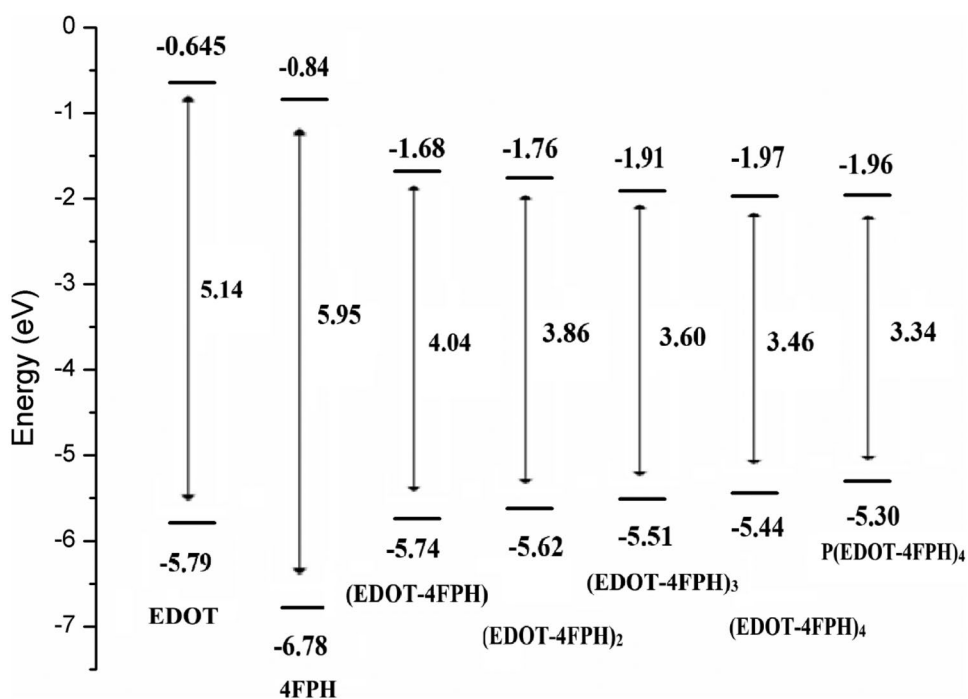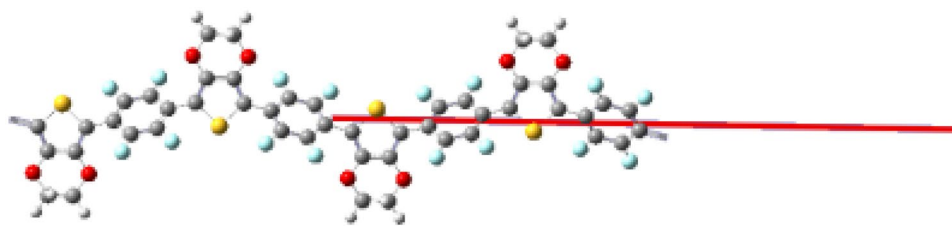synthesised by Direct Arylation Polymerization method in the presence of palladium acetate as catalyst. The reaction is presented in Scheme 2. The copolymer prepared was soluble in organic solvents like THF, CHCl$_3$, DMSO and Chlorobenzene. From Gel permeation chromatography, P(EDOT-4FPH) showed a number average and weight average molecular weight of 4720 Da and 4750 Da respectively and a dispersity value of 1.007 (Fig. S3 supporting information). Structural characterization of the copolymer was performed by FT-IR and ^{1}H NMR spectra. FT-IR spectrum of the copolymer is illustrated in (Fig. S4 supporting information). The characteristic bands appeared at 1356 cm^{-1} which represented the C-F stretching frequency and the bands observed at 1202 cm^{-1} and 1065 cm^{-1} corresponded to the C–O–C stretching frequencies. Besides these, vibrations at 3426 cm^{-1}, 2920 cm^{-1} and 1620 cm^{-1} exhibited the aromatic C-H stretching, aliphatic C-H stretching and C=C stretching frequencies respectively. ^{1}H NMR spectrum showed a broad peak at 4.34—4.57 which corresponded to –OCH$_2$ protons present in the copolymer (Fig. 4), whereas in the case of the monomer, it appeared as a sharp peak. EDX spectrum showed the presence of elements S, F, O, C in the synthesized polymer (Fig. 5).

Electrochemical studies

The electrochemical behaviour of the copolymer P(EDOT-4FPH) was studied by cyclic voltammetry (CV), differential pulse voltammetry (DPV) and square wave voltammetry (SWV). Electrochemical measurements were performed to determine the Highest occupied molecular orbital (HOMO) and Lowest unoccupied molecular orbital (LUMO) energy levels of the copolymer. The electrochemical properties of P(EDOT-4FPH) are summarized in Table 2.
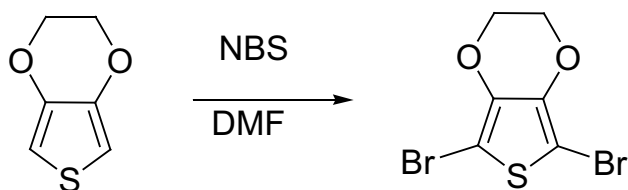
The onset of oxidation obtained from cyclic voltammetry, differential pulse voltammetry and square wave voltammetry were 1.02 V, 0.93 V, and 0.90 V respectively. Corresponding HOMO energy levels were calculated using the equation, HOMO = -(4.71 + Eox^{onset}) where Eox^{onset} stands for the onset value of oxidation potential and LUMO energy levels were obtained from the onset of reduction observed at –0.79 V, -0.78 V and -0.74 V respectively for cyclic voltammetry, differential pulse voltammetry and square wave voltammetry. Equation for the calculation of LUMO energy level is given by LUMO = -(4.71 + Ered^{onset}). Here, Ered^{onset} represents the onset value of the reduction potential [54]. Hence the electrochemical band gaps were calculated to be 1.81 eV, 1.71 eV and 1.64 eV for the copolymer P(EDOT-4FPH). Electrochemical band gap observed for the copolymer is lower in comparison with the reported E$_g$ values of 2.14 eV and 2.64 eV for P(EDAN) [27] and PEDT-PHENO [58] respectively. The lower band gap obtained for the synthesized polymer indicated enhanced electron transporting properties in the conjugated backbone due to the increase in the conjugation length. The experimental results showed some deviation from the theoretically predicted values. This is because, mostly, the theoretically predicted band gaps are used for the isolated gas-phase chains and also, the solid-state effects such as polarization effects and intermolecular packing forces are omitted [55, 56].

Thermal properties

Information regarding the thermal stability of the synthesized copolymer P(EDOT-4FPH) was gathered from the Thermogravimetric analysis. The TG-DTG curves.

estimate the mass loss that is associated with the degradation processes. From the Fig. 6, it was clear that the copolymer was having a single degradation pattern. The thermogram initially showed a weight loss of 4% due to the loss of moisture from the polymer. The onset of degradation happened at 348 °C with a weight loss of 10% that corresponded to the point where the copolymer decomposition was initiated and the degradation reached a maximum at 393 ºC, the first inflection point in the TG curve, corresponding to the peak in the derivative curve

Scheme 1 Synthesis of Br-EDOT-Br

Scheme 2 Synthesis of P(EDOT-4FPH)
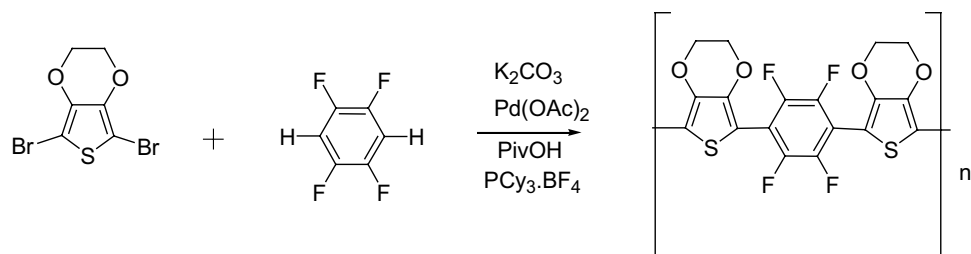
where the major decomposition of the polymer backbone occurred. The higher thermal stability of P(EDOT-4FPH) is comparable with the P(EDOT) (390 °C) [57]. Excellent thermal stability of the copolymer permits it for device fabrication since it resists the decadence and deformations it may face during the device fabrication procedures.
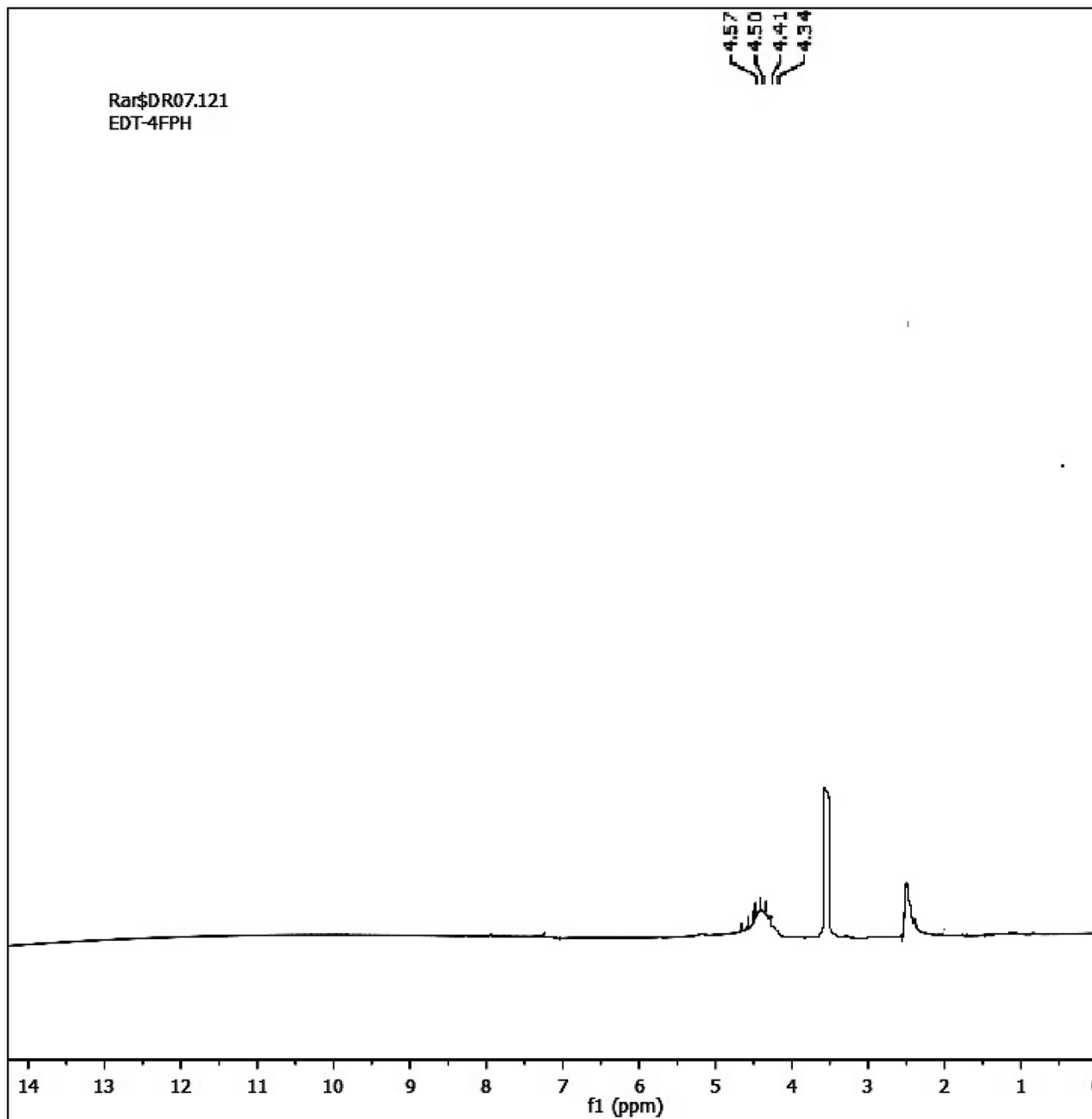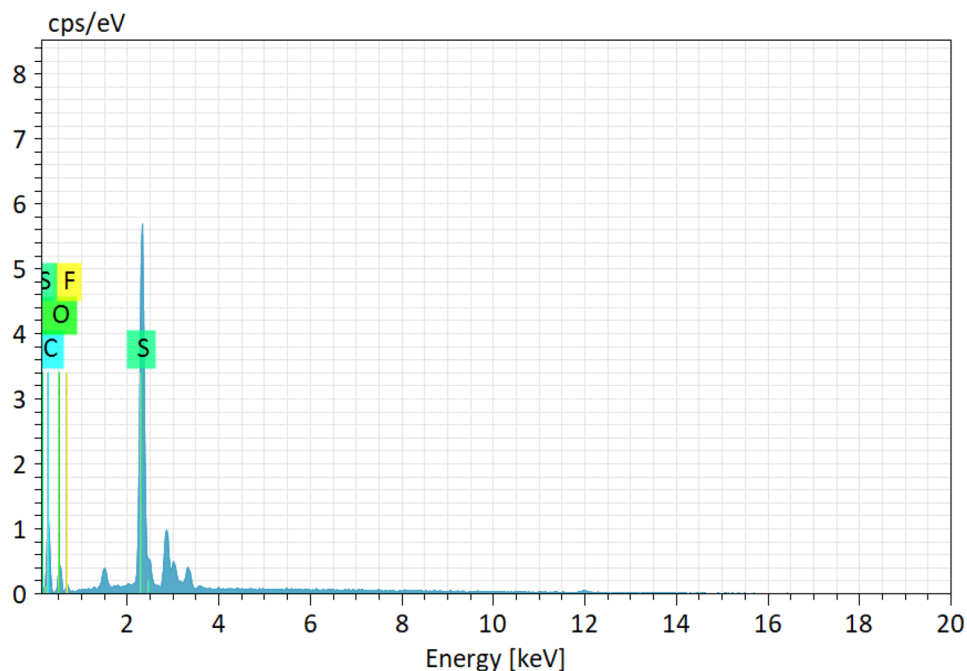

Fig. 4 ^{1}H NMR Spectrum of P(EDOT-4FPH)

Fig. 5 EDX spectrum of P(EDOT-4FPH)

Optical properties

The UV–Vis absorption spectrum of the copolymer was examined in CHCl₃ solution and as thin film which is illustrated in Fig. 7. λ_{max} values observed for the copolymer P(EDOT-4FPH) in chloroform solution and thin-film were around 500 nm. Red shift of 191 nm is observed for the copolymer P(EDOT-4FPH) in comparison with the reported π- conjugated trimer of EDOT-tetrafluorobenzene –EDOT with maximum absorption at 309 nm [33]. Thin-film of the copolymer was obtained from chloroform. Maximum absorption of the copolymer at 500 nm represented the charge transfer transition from donor to acceptor. The broadness of the peak is caused by the increased delocalization of π-electrons over the conjugated backbone. The copolymer exhibited absorption onset at 586 nm. Based on the respective onset absorption of the copolymer, the optical band gap

was estimated to be 2.05 eV, comparable with the reported optical band gap values of 2.16 eV, 1.95 eV and 1.98 eV respectively for P(EDAN), P(EDBI) and P(EDTP) [27], and lower in correlation with the optical band gap values of the copolymers PEDT-PHENO with 2.26 eV [58], tetrafluorobenzene and dialkoxybenzodithiophene based copolymer with 2.2 eV [17]. The optical band gap is well correlated with the bandgap obtained from electrochemical studies, though some deviations still exist. The difference in the mechanism of electrochemical processes and optical excitation was responsible for this deviation. In the case of optical excitation, there occurs the formation excitons (bound

Table 2 HOMO–LUMO energy levels obtained from cyclic voltammetry (**a**), differential pulse voltammetry (**b**) and Square wave voltammetry (**c**)

Polymer	Onset of oxidation (V)	HOMO (eV)	Onset of reduction (V)	LUMO (eV)	Band gap (eV)
P(EDOT-4FPH)	1.02[a]	−5.73	−0.79[a]	−3.92	1.81[a]
	0.93[b]	−5.64	−0.78[b]	−3.93	1.71[b]
	0.90[c]	−5.61	−0.74[c]	−3.97	1.64[c]

[a] Cyclic voltammetry

[b] Differential pulse voltammetry

[c] Square wave voltammetry
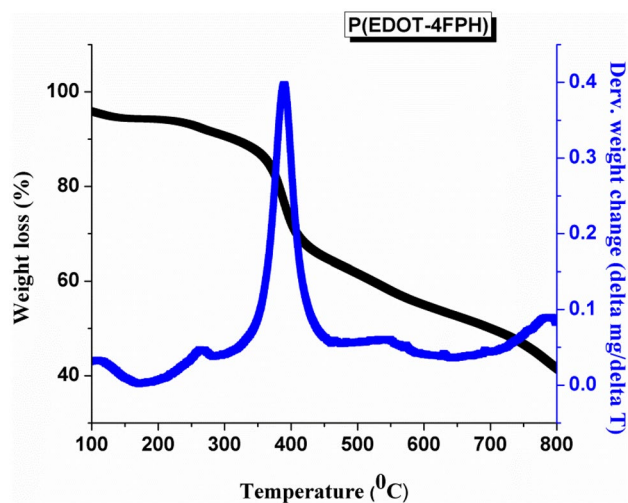
Fig. 6 TG-DTG curve of P(EDOT-4FPH)

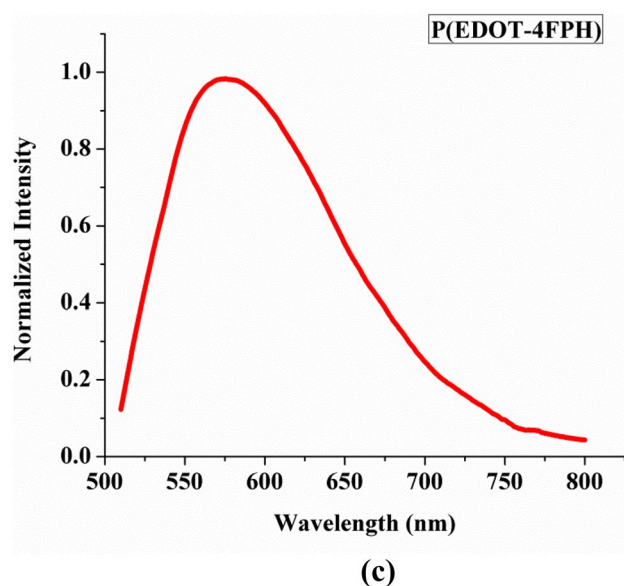**Fig. 7** UV–Vis Spectrum in chloroform solution (**a**) and thin film (**b**)

(a)

(b)

(c)
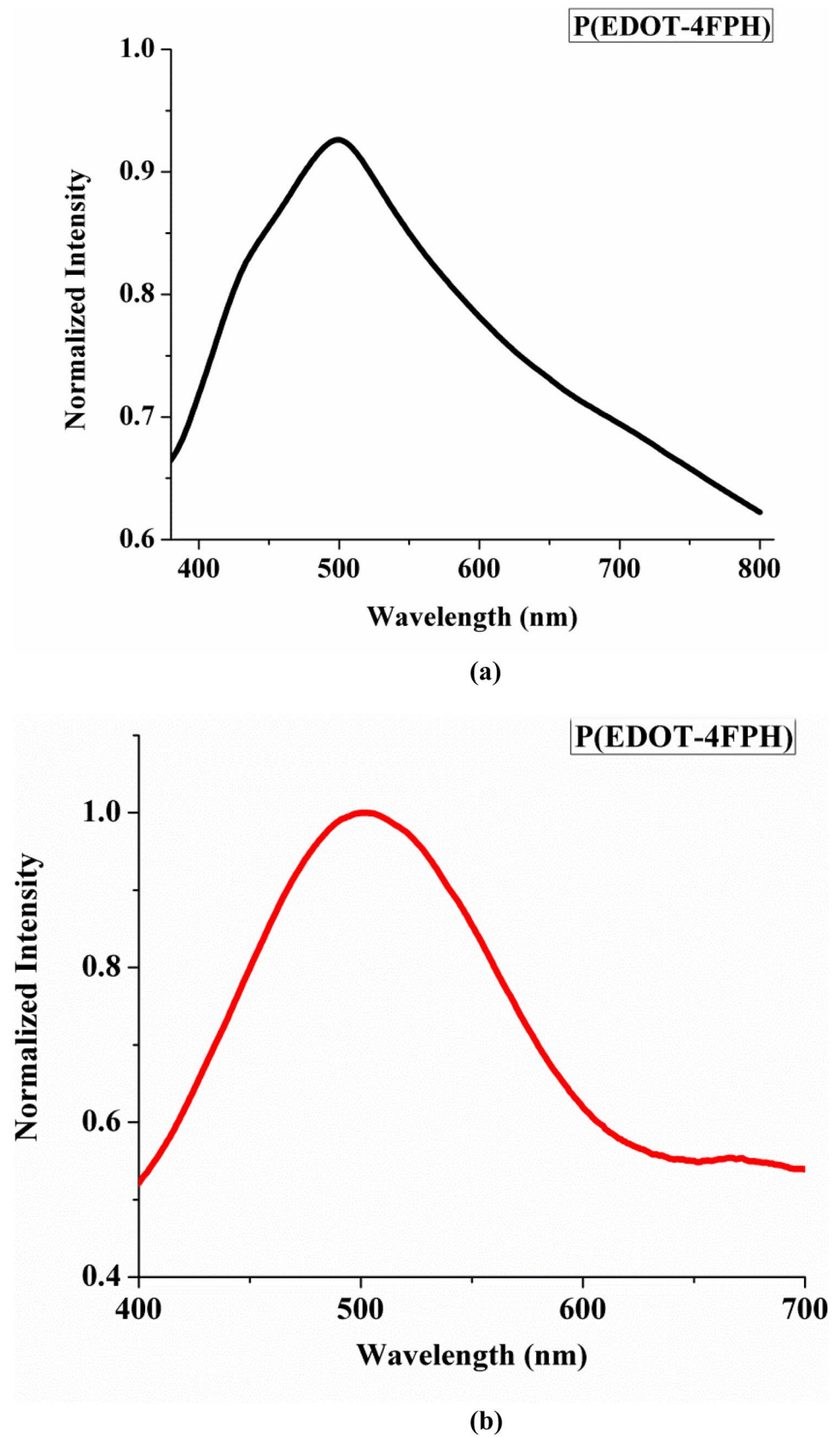
Fig. 8 Emission spectrum of P(EDOT-4FPH) in CHCl$_3$ solution

Fig. 9 Plot of integrated fluorescence intensity vs absorbance

electrons and hole pair) and where as in electrochemical process, ions are created. The low energy of excitons, compared to the ions and solvation of the ions during electrochemical experiment was reflected in the observed electrochemical band gap [29, 58] (Fig. 8).

P(EDOT-4FPH) displayed a fluorescence emission maximum at 576 nm. The wavelength used for exciting the polymer molecule was the absorption maximum observed in the UV–Vis spectrum, 500 nm. There occurred an overlap between absorption spectrum and emission spectrum by 90 nm, from 510 to 600 nm. Thus large resonance absorption was noticed. Quantum yield is the ratio of photons absorbed to photons emitted through fluorescence. To be specific, the quantum yield gives the probability of the excited state being deactivated by fluorescence rather than by another, non-radiative mechanism [59–61]. The fluorescence quantum yield of the copolymer was observed in CHCl$_3$ solution by exciting the polymer at 500 nm. Rhodamine B ($\Phi_{ST} = 0.31$ in water) [62] was used as the standard sample for the estimation of quantum yield of the polymer. Plotting a graph of integrated fluorescence intensity vs absorbance of the copolymer solution (Fig. 9) calculated the relative quantum yield using the Eq. (1) [63, 64].

$$\Phi_X = \Phi_{ST} \left(\frac{Gradx}{Gradst} \right) (\eta_X^2 / \eta_{ST}^2) \qquad (1)$$

where the subscripts Φ_{ST} and Φ_X denote the fluorescence quantum yield of the standard and the polymer respectively; Grad is the gradient from the plot of integrated fluorescence intensity vs absorbance, and η is the refractive index of the solvent. The Quantum yield achieved for P(EDOT-4FPH) is
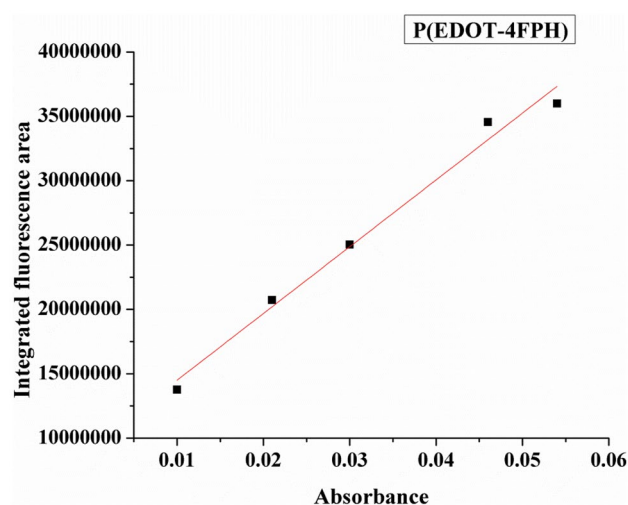
0.37 (Table 3). Low quantum yield obtained for the copolymer can be attributed due to the presence of FRET.

Time-resolved fluorescence measurements

Time-resolved fluorescence spectroscopy is used to study the lifetime decay of the excited state of the copolymer, which was not influenced by the concentration of the fluorophore, intensity of the illumination and the pathlength of the light. The polymer was excited by a flashlight and monitored the fluorescence as a function of time and emission from the copolymer could be examined by this method on nanosecond range [65, 66]. The copolymer P(EDOT-4FPH) was excited at 450 nm and the lifetime obtained was not well fitted with the single exponential decay, because of the various fluorescence fractions present with a specific lifetime. The copolymer displayed a bi-exponential lifetime decay of 0.55 ns (Table 3). The rate constant for radiative (K$_r$) and non-radiative (K$_{nr}$) processes can be estimated from the resultant average lifetime and quantum yield of the copolymer by using Eq. (2). The values are shown in Table 3 and Fig. 10.

$$K_R = \Phi_F / \tau \text{ and } K_{NR} = \left(\frac{1}{\tau} \right) - \left(\frac{\Phi F}{\tau} \right) \qquad (2)$$

P(EDOT-4FPH) excited at 450 nm presented a variation in the fluorescence lifetime decay performed in solvents of varying polarity [67] and the decay observed was bi-exponentially fitted (Fig. 11). Average lifetime values of the copolymer observed in distinct polarities are compiled in Table 3. Data indicated the dependence of fluorescence decay of the copolymer on solvent polarity in such way that the average life time value of the P(EDOT-4FPH) got

Table 3 Quantum yield, Radiative constant, non-Radiative constant, Average lifetime values of the copolymer observed in chloroform solution and Average life time values under distinct polarities

Solvent	χ^2	τ_1(ns)	α_1 (%)	τ_2 (ns)	α_2 (%)	Average life time τ (ns)	Quantum Yield	K_r (s^{-1})	K_{nr} (s^{-1})
Chloroform	1.10	2.21	3	0.51	97	0.55	0.37	6.65×10^8	1.13×10^9
Toluene	1.003	0.49	99	2.49	1	0.50	-	-	-
Toluene + Acetonitrile (80:20)	1.21	2.01	2	0.54	97	0.58	-	-	-
Toluene + Acetonitrile (60:40)	1.24	2.17	4	0.54	95	0.61	-	-	-
Acetonitrile	1.24	1.90	5	0.67	94	0.74	-	-	-

increased from non-polar to polar solvent. This may be due to the decrease in the non-radiative deactivation on increasing the polarity of the solvent [68].

Solvatochromic studies

Solvatochromism is the colour change that emerges due to the difference in the polarity of solvents. It is evident from the changes, either in the shape, position and intensity of the UV–Vis absorption and fluorescence spectrum. Solvatochromic studies can bring information regarding the geometric and electronic structure of the conjugated polymers. The present study was the observation regarding the shifts seen in the absorption and emission spectra of the synthesized copolymer P(EDOT-4FPH) in a binary solvent mixture of polar acetonitrile and non-polar toluene in varying proportions (Fig. 12). Toluene/acetonitrile mixtures were prepared at different ratios of individual solvents in a way that the solution switched from non-polar to polar with the gaining weight fractions of acetonitrile. The polarity of the binary mixtures was evaluated from the

solvent polarity parameter E_T^N, calculated using the standard 2,6-Diphenyl-4-(2,4,6-triphenyl-1-pyridinio) phenolate (Reichardt's dye) which exhibited a large effect of solvatochromism [69–71]. The plot of Stokes shift against solvent polarity parameter E_T^N implies the linear interaction of the copolymer with the solvents, given in Fig. 13 and the data are presented in Table 4.

It was observed that, both the absorption and emission exhibited dependence on the solvent polarity which appeared as a hypsochromic/blue shift in the case of absorption (negative solvatochromism) where λ_{max} was decreased from 499 to 488 nm, as the energy gap between the HOMO and LUMO was increased due to the effect of polarity of the solvent and Bathochromic/ redshift (positive solvatochromism) in the case of emission where λ_{max} was increased from 564 to 612 nm, by the impact of solvent polarity, as seen in (Table 4). The average lifetime of the copolymer got increased when the solvent became more polar in nature. There occurred less shift on the absorption spectra by the solvent polarity change indicating that the energy distribution of the ground state was
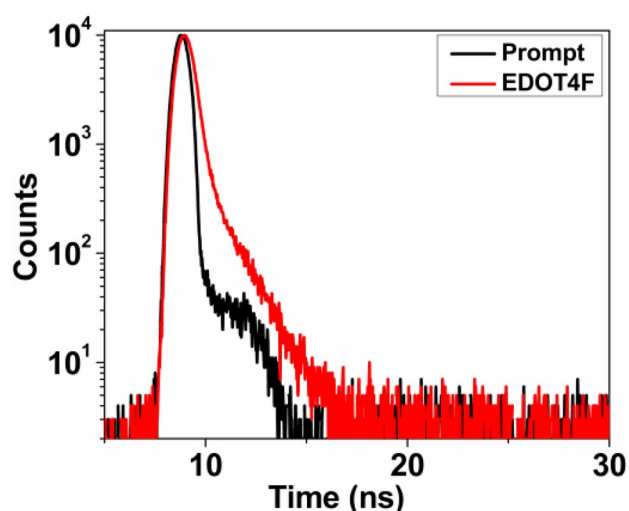

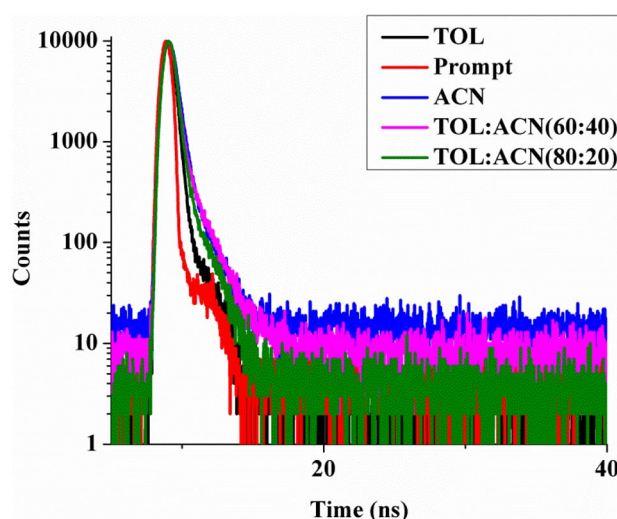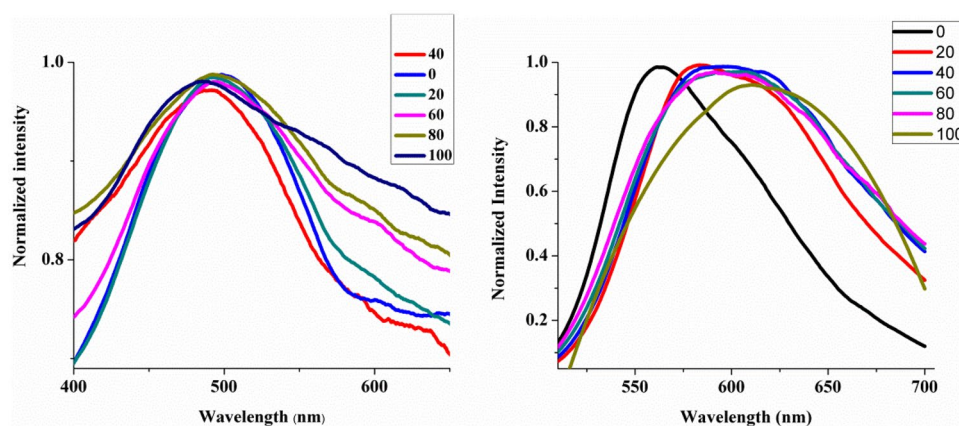**Fig. 10** Time-resolved fluorescence spectrum of P(EDOT-4FPH) in chloroform

Fig. 11 Time-resolved fluorescence spectra of P(EDOT-4FPH) in different solvents

not affected much, as it was having a less polar nature in the ground state. Whereas for the emission, there was a large shift which implied that the excited state energy levels were more influenced by the solvent polarity. For the copolymer, P(EDOT-4FPH), large Stoke's shift value (ν^{abs}- ν^{emi}) was observed from 2310 cm^{-1} to 4152 cm^{-1} by the different ratios of binary mixtures on comparing it to the reported Stoke's shift value of P(EDAN) from 3721 cm^{-1} to 4409 cm^{-1}, where EDOT plays the role of donor and anthracene act as the acceptor unit [27]. This indicated the charge transfer occurred between donor and acceptor units of the polymer [72].

Nonlinear optical properties

Third order non-linear optical properties of the copolymer P(EDOT-4FPH) were evaluated using the open-aperture Z-scan technique at 532 nm [73] in DMSO solvent. The OA trace of the copolymer in DMSO solvent was recorded at different laser fluence as shown in Fig. 14.
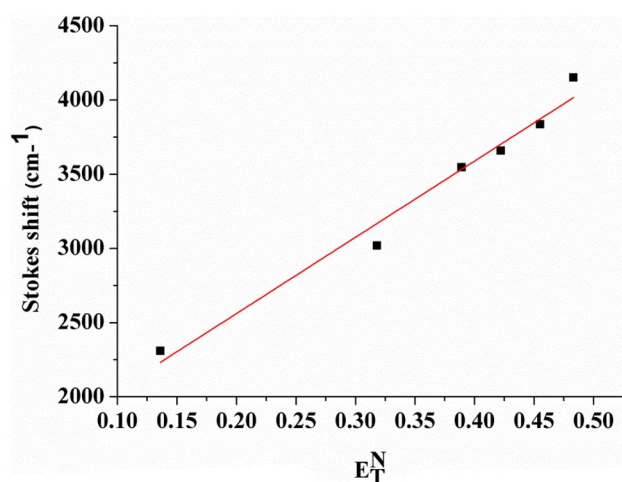
The copolymer showed a Reverse Saturable Absorption curve with positive NLO absorption coefficient β and the experimentally obtained curve was well fitted with the theoretically obtained curve from the Two-photon absorption theory. By fitting the experimental Z-scan data using the Eq. (3), β value was calculated.

$$T(z) = \frac{C}{q_0 \sqrt{\pi}} \int_{-\infty}^{\infty} ln(1 + q_0 e^{-t^2}) dt \tag{3}$$

$q_{0(z,r,t)} = \beta I_0(t) L_{eff}$ and $L_{eff} = (1 - {}^{e^{-al}} /_{\alpha})$ is the effective thickness with linear absorption coefficient α, and 'I'$_0$ is the irradiance at focus.

Non-linear absorption coefficient values obtained for the copolymer were in the order of 10^{-9} m/W, which indicated that the copolymer was in the range of a semiconductor, which was found to be higher in the case of 18 μJ irradiation and the strong nonlinearity was observed for the copolymer even at lower laser fluencies in comparison with the reported EDOT based copolymers which showed strong non-linearity at 112 μJ [29], which resulted due to the strong donor–acceptor interaction in the copolymer (Table 5).

Fig. 13 Stokes shift against solvent polarity parameter

Table 4 Solvent polarity parameter corresponding to the binary solvent mixture at different volume fractions of acetonitrile and the corresponding absorption and emission maxima

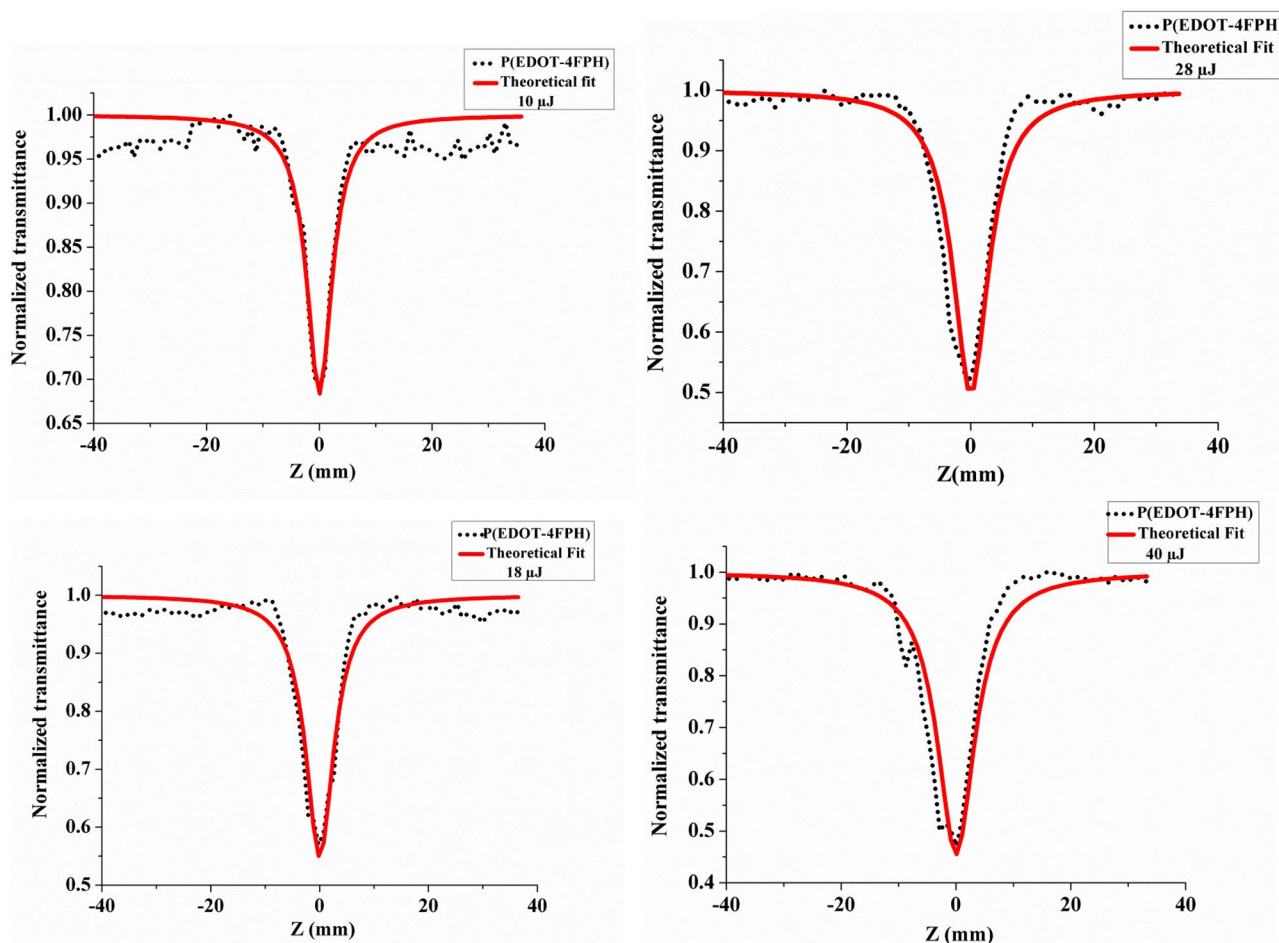| Volume Fraction of Acetonitrile (%)	E_T^N	λ_{max}^{abs}(nm)	$\lambda_{max}^{emission}$ (nm)	Stokes shift (cm^{-1})
0	0.136	499	564	2310
20	0.318	495	582	3020
40	0.389	492	596	3547
60	0.422	492	600	3659
80	0.455	491	605	3838
100	0.483	488	612	4152

Fig. 14 Open-aperture Z-scan traces of P(EDOT-4FPH) in DMSO at 10 μJ,18 μJ,28 μJ and 40 μJ with the red line as the theoretical fit

Optical power limting

Non-linearity in absorption shown by the polymer P(EDOT-4FPH), made it possible to be an optical limiting material, which permitted light at low intensities and behaved as an opaque material at high input [74]. The property of optical limiting was observed by measuring non-linear transmission at various input intensities. Open –aperture Z-scan measurements conducted at 532 nm was used to study the optical limiting property. Figure 15 depicts the optical limiting behaviour observed for the copolymer. It is clear that at low input intensity, the copolymer obeyed Beer'law, but it behaved differently when it approached the optical limiting threshold; it started to behave like an optical limiting material. The observed optical limiting threshold values for the copolymer at different laser intensities, 10 μJ, 18 μJ, 28 μJ and 40 μJ were 0.005 GW/cm^2, 0.009 GW/cm^2, 0.016 GW/cm^2 and 0.027 GW/cm^2 respectively (Fig. 15) which were lower than the reported optical limiting threshold values of the EDOT- Quinoxaline and chalcogenadiazole copolymers, that showed optical limiting threshold values in the range of 0.2 -0.4 GW/cm^2 [28, 29]. The lower optical limiting

Table 5 Non-linear absorption coefficient, Intensity and L_{eff} for the copolymer at different pulse energies

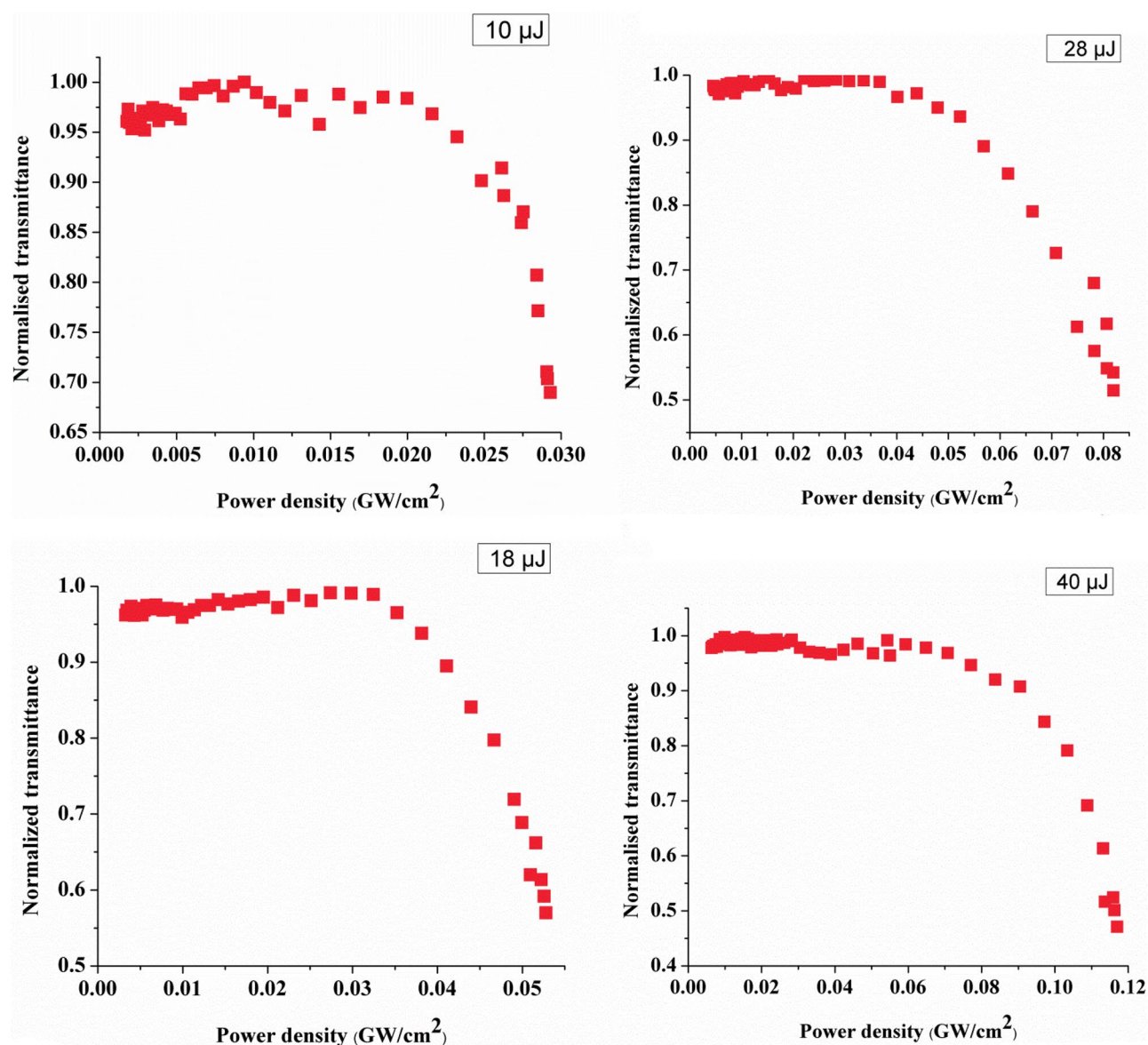| Sample code	Pulse Energy (μJ)	Intensity (J/m^2)	L_{eff} (effective thickness) (mm)	Beta (m/W) (Non- linear absorption coefficient)
P(EDOT-4FPH)	10	2.93×10^{11}	9.88×10^{-4}	3.63×10^{-9}
P(EDOT-4FPH)	18	5.28×10^{7}	9.88×10^{-4}	3.86×10^{-9}
P(EDOT-4FPH)	28	8.21×10^{7}	9.88×10^{-4}	3.14×10^{-9}
P(EDOT-4FPH)	40	1.17×10^{12}	9.88×10^{-4}	2.67×10^{-9}

Fig. 15 Optical limiting curves of P(EDOT-4FPH) at different input intensities

threshold values indicated the better optical limiting effect of the copolymer. At the low applied intensity of 10 µJ, the copolymer produced an excellent optical limiting effect with a 0.005 GW/cm^2 optical threshold value.

Conclusion

Donor–Acceptor copolymer, P(EDOT-4FPH) was designed and synthesized by the Direct arylation polymerization method. Theoretical investigations were carried out using Gaussian 09 with two levels of density functional theory B3LYP and HSE06. Results obtained from the HSE06/6-31G (d,p) basis set were more close to the experimental data

even though there existed some variations, as the predicted band gaps were for the isolated gas phase chains and also, the solid state effects such as intermolecular packing forces and polarization effects were neglected in the theoretical studies. The copolymer was characterized by FT-IR, ^{1}H NMR, TGA, EDAX etc. The electrochemical band gap obtained for the copolymer by CV was observed to be 1.81 eV and optical band gap was 2.05 eV. The deviations observed in the optical and electrochemical band gaps can be attributed to the difference in the mechanism of electrochemical process and optical excitation. The copolymer exhibited a positive solvatochromism and an increase in the value of average lifetime with the increase in solvent polarity was observed. The third-order non-linear optical properties were studied

by the OA Z-scan technique at 532 nm. It showed RSA non-linear absorption with a lower optical limiting threshold of 0.005 GW/cm^2 at 10 μJ. Thus, the copolymer developed is a promising material for optoelectronic applications.

Data availability All data analyzed in this study are included in this article. If more information is needed, it can be available on request from the corresponding author.

Declarations

Conflict of interest The authors declare that they have no conflict of interest.

References

1. Li L, Yu Y, Yu J (2021) Semiconductor solar photocatalysts, organic semiconductor photocatalysts, Wiley 325–364

2. Hopkins J, Fidanovski K, Lauto A, Mawad D (2019) All-organic semiconductors for electrochemical biosensors: an overview of recent progress in material design. Front Bioeng Biotechnol 7:237–245

3. Lete C, Lupu S, Lakard B, Hihn JY, Campo FJ (2015) Multi-analyte determination of dopamine and catechol at single-walled carbon nanotubes – Conducting polymer – Tyrosinase based electrochemical biosensors. J Electroanal Chem 744:53–61

4. Zhang H, Ming S, Liang Y, Feng L, Xu T (2020) A multi-color electrochromic material based on organic polymer. Int J Electrochem Sci 15:1044–1057

5. Zhang L, Jamal R, Zhao Q, Zhang Y, Wang M, Abdiryim T (2015) Polym Compos 37:2884–2896

6. Nelson J (2011) Polymer: fullerene bulk heterojunction solar cells. Mater Today 14:1369–7021

7. Nattestad A, Perera I, Spiccia L (2016) Developments and prospects for photocathodic and tandem dye-sensitized solar cells. J Photochem Photobiol C 28:44–71

8. Roncali J (2007) Molecular engineering of the band gap of π-conjugated systems: facing technological applications. Macromol Rapid Commun 28:1761–1775

9. Schipper DJ, Fagnou K (2011) Direct arylation as a synthetic tool for the synthesis of thiophene-based organic electronic materials. Chem Mater 23:1594–1600

10. Nohara Y, Kuwabara J, Yasuda T, Han L, Kanbara T (2014) Two-step direct arylation for synthesis of naphthalenediimide-based conjugated polymer. J Polym Sci A Polym Chem 52:1401–1407

11. Poduval MK, Burrezo PM, Casado J, López Navarrete JT, Ortiz RP, Kim T-H (2013) Novel thiophene-phenylene-thiophene fused bislactam-based donor–acceptor type conjugate polymers:

12. synthesis by direct arylation and properties. Macromolecules 46:9220–9230

13. Okutan M, Yerli Y, San SE, Yılmaz F, Gunaydın O, Durak M (2007) Dielectric properties of thiophene based conducting polymers. Synth Met 157:368–373

14. Park JH, Jung EH, Jung JW, Jo WH (2013) A fluorinated phenylene unit as a building block for high performance n-type semiconducting polymer. Adv Mater 25:2583–2588

15. Araujo MHD, Matencio T, Donnici CL, Calado HDR (2020) Electrical and spectroelectrochemical investigation of thiophene-based donor-acceptor copolymers with 3,4-ethylenedioxythiophene. Polimeros 30:1–10

16. Fiket L, Cevi MB, Brk L, Zagar P, Horvat A, Katan Z (2022) Intrinsically stretchable poly(3,4-ethylenedioxythiophene) conducting polymer film for flexible electronics. Polymers 14:2340–2356

17. Yang Y, Deng H, Fu Q (2020) Recent progress on PEDOT: PSS based polymer blends and composites for flexible electronics and thermoelectric devices. Mater Chem Front 4:3130–3152

18. Nitti A, Debattista F, Abbondanza L, Bianchi G, Po R, Pasini D (2017) Donor-acceptor conjugated copolymers incorporating tetrafluorobenzene as the π-electron deficient unit. J Polym Sci A Polym Chem 55:1601–1610

19. Broll S, Nübling F, Luzio A, Lentzas D, Komber H, Caironi M, Sommer M (2015) Defect-analysis of high electron mobility diketopyrrolopyrrole copolymers made by direct arylation polycondensation. Macromolecules 48:7481–7488

20. Wong S, Ma H, Jen AK-Y, Barto R, Frank CW (2003) Highly fluorinated trifluorovinyl aryl ether monomers and perfluorocyclobutane aromatic ether polymers for optical waveguide applications. Macromolecules 36:8001–8007

21. Pagliaro M, Ciriminna R (2005) New fluorinated functional materials. J Mater Chem 15:4981–4991

22. Yamazaki K, Kuwabara J, Kanbara T (2013) Synthesis of π-conjugated polymer consisting of pyrrole and fluorene units by ru-catalyzed site-selective direct arylation polycondensation. Macromol Rapid Commun 34:69–73

23. Kuwabara J, Yasuda T, Choi SJ, Lu W, Yamazaki K, Kagaya S, Han L, Kanbara T (2014) Direct arylation polycondensation for synthesis of optoelectronic materials. Polym J 24:3226–3233

24. Rudenko AE, Thompson BC (2015) Optimization of direct arylation polymerization through the identification and control of defects in polymer structure. J Polym Sci A Polym Chem 53:135–147

25. Kowalski S, Allarda S, Zilberberg K, Riedl T, Scherf U (2013) Direct arylation as simplified alternative for the synthesis of conjugated (co) polymers. Prog Polym Sci 38:1805–1814

26. Crouch DJ, Skabara PJ, Heeney M, McCulloch I, Colesc SJ, Hursthousec MB (2005) Hexyl-substituted oligothiophenes with a central tetrafluorophenylene unit: crystal engineering of planar structures for p-type organic semiconductors. Chem Comm 11:1465–1467

27. Wang Z, Li K, Zhao D, Lan J, You J (2011) Palladium-catalyzed oxidative CH/CH cross-coupling of indoles and pyrroles with heteroarenes. J Am Chem Soc 50:5365–5369

28. Pillai JJ (2019) Development of donor-acceptor low band gap polymers for photoconducting and non-linear optical applications: theoretical design and synthesis. Ph.D Thesis, Cochin Univ Sci Technol

29. Narayanan S, Raghunathan SP, Poulose AC, Mathew S, Sreekumar K, Kartha CS, Joseph R (2015) Third-order nonlinear optical properties of 3,4- ethylenedioxythiophene copolymers with chalcogenadiazole acceptors. New J Chem 39:2795–2806

30. Narayanan S, Raghunathan SP, Mathew S, Kumar MVM, Abbas A, Sreekumar K, Kartha CS, Joseph R (2015) Synthesis and third-order nonlinear optical properties of low band gap

3,4-ethylenedioxythiophene-quinoxaline copolymers. Eur Polym J 64:157–169

30. Kempe F, Riehle F, Komber H, Matsidik R, Walter M, Sommer M (2020) Semifluorinated, kinked polyarylenes via direct arylation polycondensation. Polym Chem 11:6928–6934

31. Baby AM, Theresa LV, Sreekumar K (2022) Theoretical design, synthesis and third-order non-linear optical properties of thiophene and tetrafluorobenzene based low band gap conducting polymers. J Mol Struct 1265:133301–133319

32. Cui X, Xio C, Jiang W, Wang Z (2019) Alternating tetrafluorobenzene and thiophene units by direct arylation for organic electronics. Chem Asian J 14:1443–1447

33. Kharandiuk T, Hussien EJ, Cameron J, Petrina R, Findlay NJ, Naumov R, Klooster WT, Coles SJ, Ai Q, Goodlett S, Risko C, Skabara PJ (2019) Noncovalent close contacts in fluorinated thiophene−phenylene− thiophene conjugated units: understanding the nature and dominance of O···H versus S···F and O···F interactions with respect to the control of polymer conformation. Chem Mater 31:7070–7079

34. Becke AD (1993) Density-functional thermochemistry. III. The role of exact exchange. J Chem Phys 98:5648–5652

35. Xu X, William A (2004) Goddard, the X3LYP extended density functional for accurate descriptions of nonbond interactions, spin states, and thermochemical properties. Proc Natl Acad Sci 101:2673–2677

36. Burke K, Perdew JP, Wang Y, Dobson JF, Vignale G, Das MP (1998) Electronic density functional theory: recent progress and new directions, plenum press

37. Parr RG, Yang W (1989) Density-functional theory of atoms and molecules. Int J Quantum Chem 47:101–101

38. Kornobis K, Kumar N, Lodowski P, Jaworska M, Piecuch P, Lutz JJ, Wong BM, Kozlowski PM (2013) Electronic structure of the S1 state in methylcobalamin: insight from CASSCF/MC-XQDPT2, EOM-CCSD, and TD-DFT calculations. J Comput Chem 113:479–488

39. Kumar N, Alfonso-Prieto M, Rovira C, Lodowski P, Jaworska M, Kozlowski PM (2011) Role of the axial base in the modulation of the Cob (I) alamin electronic properties: insight from QM/MM, DFT, and CASSCF calculation. J Chem Theory Comput 7:1541–1551

40. Bryan MW, Manuel P, Fabio DS (2009) Optical and magnetic properties of boron fullerenes. Phys Chem Chem Phys 11:4523–4527

41. Kim K, Jordan KD (1994) Comparison of density functional and MP2 calculations on the water monomer and dimer. J Phys Chem 98:10089–10094

42. Vosko SH, Wilk L, Nusair M (1980) Structural and electronic properties of Bixo3 (X= Mn, Fe, Cr). J Phys 58:1200–1211

43. Devlin FJ, Finley JW, Stephens PJ, Frisch MJ (1995) Ab initio calculation of vibrational absorption and circular dichroism spectra using density functional force fields, a comparison of local, nonlocal, and hybrid density functionals. J Phys Chem 95:16883–16902

44. Dobson JF, Vignale G, Das MP (2013) Electronic density functional theory: recent progress and new directions. Springer Science & Business Media 147–149

45. Frisch MJ, Trucks GW, Schlegel HB, Scuseria GE, Robb MA, Cheeseman JR, Scalmani G, Barone V, Mennucci B, Petersson GA, Nakatsuji H, Caricato M, Li X, Hratchian HP, Izmaylov A, Bloino J, Zheng G, Sonnenberg JL, Hada M, Ehara M, Toyota K, Fukuda R, Hasegawa J, Ishida M, Nakajima T, Honda Y, Kitao O, Nakai H, Vreven T, Montgomery JA, Peralta JE, Ogliaro F, Bearpark M, Heyd JJ, Brothers E, Kudin KN, Staroverov VN, Kobayashi R, Normand J, Raghavachari K, Rendell A, Burant JC, Iyengar SS, Tomasi J, Cossi M, Rega N, Millam NJ, Klene M, Knox JE, Cross JB, Bakken V, Adamo C, Jaramillo J, Gomperts R, Stratmann RE, Yazyev O, Austin AJ, Cammi R, Pomelli C,

Ochterski JW, Martin RL, Morokuma K, Zakrzewski VG, Voth GA, Salvador P, Dannenberg JJ, Dapprich S, Daniels AJ, Farkas O, Foresman JB, Ortiz JV, Cioslowski J, Fox DJ (2009) Gaussian, Inc., Wallingford CT. Gaussian 09, Revision B02

46. Marom N, Tkatchenko A, Rossi M, Gobre VV, Hod O, Scheffler M (2011) Dispersion Interactions with Density-Functional Theory: Benchmarking Semiempirical and Interatomic Pairwise Corrected Density Functionals. J Chem Theory Comput 7:3944–3951

47. Donat-Bouillud A, Levesque I, Tao Y, D'Iorio M, Beaupré S, Blondin P, Ranger M, Bouchard J, Leclerc M (2000) Light-emitting diodes from fluorene-based-conjugated polymers. Chem Mater 12:1931–1936

48. Liégault B, Lapointe D, Caron L, Vlassova A, Fagnou K (2009) Establishment of broadly applicable reaction conditions for the palladium-catalyzed direct arylation of heteroatom-containing aromatic compounds. J Org Chem 74:1826–1834

49. Leclerc M, Brassard S, Beaupré S (2020) Direct (hetero) arylation polymerization: towards defect-free conjugated polymers. Polym J 52:13–20

50. Gobalasingham NS, Thompson BC (2018) Direct arylation polymerization: a guide to optimal conditions for effective conjugated polymers. Prog Polym Sci 83:135–201

51. Hayashi S, Yamamoto S, Koizumi T (2018) Study on direct arylation of bithiophene with dibromoxanthene: detection of polymer, oligomeric and cyclic byproducts and easy separation of the polymer. Mater Today Commun 17:259–265

52. Huang J, Lin Z, Feng W, Wang W (2019) Synthesis of bithiophene-based D-A1-D-A2 terpolymers with different a2 moieties for polymer solar cells via direct arylation. Polymers 11:55–66

53. Narayanan S (2015) Design and synthesis of donor-acceptor low band gap copolymers for photoconducting and non-linear optical applications: theoretical design and synthesis. Ph.D Thesis, Cochin Univ Sci Technol

54. Bredas JL, Silbey R, Boudreux DX, Chance RR (1983) Chain-length dependence of electronic and electrochemical properties of conjugated systems: polyacetylene, polyphenylene, polythiophene, and polypyrrole. J Am Chem Soc 105:6555–6559

55. Puschning P, Ambrosch-Draxl C, Heimel G, Zojer E, Resel R, Leising G, Kriechbaum M, Graupner W (2001) Pressure studies on the intermolecular interactions in biphenyl. Synth Met 116:327–331

56. Eaton VJ, Steele DJ (1973) Dihedral angle of biphenyl in solution and the molecular force field. J Chem Soc Faraday Trans 69:1601–1608

57. Kiebooms R, Aleshin A, Hutchison K, Wudl F, Heeger A (1999) Doped poly(3,4-ethylenedioxythiophene) films: thermal, electromagnetical and morphological analysis. Synth Met 101:436–437

58. Kumar M (2012) Design and synthesis of conjugated polymers for photovoltaic and chemosensor applications. Ph.D Thesis, Cochin Univ Sci Technol

59. Bindhu CV, Harilal SS, Varier GK, Issac RC, Nampoori VPN, Vallabhan CPG (1996) Measurement of the absolute fluorescence quantum yield of rhodamine B solution using a dual-beam thermal lens technique. J Phys D Appl Phys 29:1074–1079

60. Lakowicz JR (1999) Principles of Fluorescence Spectroscopy, Edition 2nd. Kluwer, Academic/Plenum Publishers

61. Jameson DM, Croney JC, Moens P (2003) Basic concepts in fluorescence, fluorescence: practical aspects and some anecdotes. Methods Enzymol 360:1–43

62. Dhami S, de Mello AJ, Rumbles G, Bishop SM, Phillips D, Beeby A (1995) Phthalocyanine fluorescence at high concentration: dimers or reabsorption effect? Photochem Photobiol 61:341–346

63. Williams ATR, Winfield SA, Miller JN (1983) Relative fluorescence quantum yields using a computer controlled luminescence spectrometer. Analyst 108:1067–1071

64. Narayanan S, Abbas A, Anjali CP, Xavier S, Sudha Kartha C, Devaky KS, Sreekumar K, Joseph R (2018) Low band gap

donor-acceptor phenothiazine copolymer with triazine segment: design, synthesis and application for optical limiting devices. J Lumin 198:449–456

65. Suhling K, French PMW, Phillips D (2005) Time-resolved fluorescence microscopy. Photochem Photobio Sci 4:13–22

66. Millar DP (1996) Time-resolved fluorescence spectroscopy. Curr Opin Struct Biol 6:637–642

67. Magde D, Rojas GE, Seybold P (1999) Solvent dependence of the fluorescence lifetimes of xanthene dyes. Photochem Photobiol 70:737–744

68. Siddlingeshwar SB, Thomas A, Kirilova EM, Divakar DD, Alkheraif AA (2019) Experimental and theoretical insights on the effect of solvent polarity on the photophysical properties of a benzanthrone dye. Spectrochim Acta A Mol Biomol Spectrosc 218:221–228

69. Reichardt C (2007) Solvents and solvent effects: an introduction. Org Process Res Dev 11:105–113

70. Čunderlíková B, Šikurová L (2001) Solvent effects on photophysical properties of merocyanine 540 B. Chem Phy 263:415–422

71. Xavier S, Narayanan S, Anjali CP, Sreekumar K (2019) Theoretical design, synthesis and studies on the solvatochromic behaviour of low band gap phenylenevinylene based copolymers. Eur Polym J 113:365–376

72. Banerji N, Gagnon E, Morgantini P, Valouch S, Mohebbi AL, Seo JH, Lecrec M, Heeger AJ (2012) Breaking down the problem: optical transitions, electronic structure and photoconductivity in conjugated polymer PCDTBT and in its separate building blocks. J Phys Chem 116:11456–11469

73. Van Stryland EW, Sheik-Bahae M, Said AA, Hagan DJ (1993) Characterization of nonlinear optical absorption and refraction. Prog Cryst Growth Charact Mater 27:279–311

74. He GS, Xu GC, Prasad PN, Reinhardt BA, Bhatt JC, Dillard AG (1995) Nonlinear multiphoton processes in organic and polymeric materials. Opt Lett 20:435–437